MYADM regulates Rac1 targeting to ordered membranes required for cell spreading and migration

Juan F. Aranda[a], Natalia Reglero-Real[a], Leonor Kremer[b], Beatriz Marcos-Ramiro[a], Ana Ruiz-Sáenz[a], María Calvo[c], Carlos Enrich[d], Isabel Correas[a], Jaime Millán[a,*], and Miguel A. Alonso[a,*]

[a]Centro de Biología Molecular Severo Ochoa and [b]Centro Nacional de Biotecnología Consejo Superior de Investigaciones Científicas and Universidad Autónoma de Madrid, Cantoblanco, 28049 Madrid, Spain; [c]Unidad de Microscopía Confocal Servicios Científico-técnicos and [d]Departament de Biologia Celular Immunologia i Neurociències, Institut d'Investigacions Biomèdiques August Pi i Sunyer (IDIBAPS), Facultat de Medicina Universidad de Barcelona, 08036 Barcelona, Spain

ABSTRACT Membrane organization into condensed domains or rafts provides molecular platforms for selective recruitment of proteins. Cell migration is a general process that requires spatiotemporal targeting of Rac1 to membrane rafts. The protein machinery responsible for making rafts competent to recruit Rac1 remains elusive. Some members of the MAL family of proteins are involved in specialized processes dependent on this type of membrane. Because condensed membrane domains are a general feature of the plasma membrane of all mammalian cells, we hypothesized that MAL family members with ubiquitous expression and plasma membrane distribution could be involved in the organization of membranes for cell migration. We show that myeloid-associated differentiation marker (MYADM), a protein with unique features within the MAL family, colocalizes with Rac1 in membrane protrusions at the cell surface and distributes in condensed membranes. MYADM knockdown (KD) cells had altered membrane condensation and showed deficient incorporation of Rac1 to membrane raft fractions and, similar to Rac1 KD cells, exhibited reduced cell spreading and migration. Results of rescue-of-function experiments by expression of MYADM or active Rac1L61 in cells knocked down for Rac1 or MYADM, respectively, are consistent with the idea that MYADM and Rac1 act on parallel pathways that lead to similar functional outcomes.

INTRODUCTION

Cell migration can be defined as a cyclical process of assembly/disassembly of integrin-based adhesive structures coordinated by the underlying cytoskeleton. Such adhesive turnover is usually ori-

ented toward spatiotemporal cues in the environment and mediates vital processes, such as organism development, wound repair angiogenesis, and immune responses (Ridley et al., 2003). A pathological deregulation of cell migration contributes to serious diseases like cancer and metastasis atherosclerosis and autoimmunity (Rolfe et al., 2005; Yamazaki et al., 2005).

Oriented motility requires mechanisms of compartmentalization at the plasma membrane to generate asymmetry in signaling pathways that drive forward movement at the leading edge or contraction at the back of the cell (Manes et al., 2003; Ridley et al., 2003). One such mechanism arises from the existence of membrane heterogeneity that favors the selective recruitment of protein complexes (Manes et al., 2003; Golub and Pico, 2005). Cholesterol-dependent membrane domains with varying degrees of condensation can be visualized in living cells by staining with the fluorescent probe Laurdan (Gaus et al., 2003, 2006a). Condensed membranes are probably equivalent to liquid-ordered membrane assemblies of glycolipids and cholesterol (also referred to as membrane rafts),

which are involved in recruiting specific proteins for membrane trafficking or signaling events and in forming membrane compartments, such as caveolae (Simons and Ikonen, 1997; Lingwood and Simons, 2010). The Rho-family guanosine triphosphatase (GTPase) Rac1 is distributed in ordered membranes of appropriate microviscosity (Ghosh *et al.*, 2002; del Pozo *et al.*, 2004; Vilhardt and van Deurs, 2004) and regulates spreading and actin-mediated extension of lamellipodia, where nascent adhesive structures initiate oriented movement (Ridley *et al.*, 2003; del Pozo *et al.*, 2004; Heasman and Ridley, 2008). The machinery responsible for making condensed membranes competent to recruit Rac1 has remained elusive.

Members of the MAL protein family play a role in raft membranes (Cheong *et al.*, 1999; Puertollano *et al.*, 1999; Magal *et al.*, 2009). The best documented proteins of this family (MAL, BENE, MAL2, and plasmolipin) contain four transmembrane segments expressed in a restricted range of tissues and are involved in specialized membrane-trafficking processes (Puertollano *et al.*, 1999; de Marco et al., 2001, 2002; Bosse *et al.*, 2003). Because condensed membrane domains are a general feature of the plasma membrane of all mammalian cells, we hypothesized that MAL family members with ubiquitous expression and plasma membrane distribution could be involved in the function of raft membranes for cell migration. Here we report the functional characterization of the myeloid-associated differentiation marker (MYADM), a member of the MAL family with the unique features of having eight transmembrane regions and a ubiquitous pattern of expression and of being localized at the plasma membrane. Using a combination of RNA interference and rescue-of-function experimental analysis of condensed domains by Laurdan staining and isolation of detergent-insoluble membranes and different functional analyses, we found MYADM to be important for the organization of membrane domains crucial for appropriate targeting of Rac1 and hence for lamellipodium extension and cell motility.

RESULTS

MYADM is broadly expressed, partitions into compact membranes, and distributes to cell lamellipodia
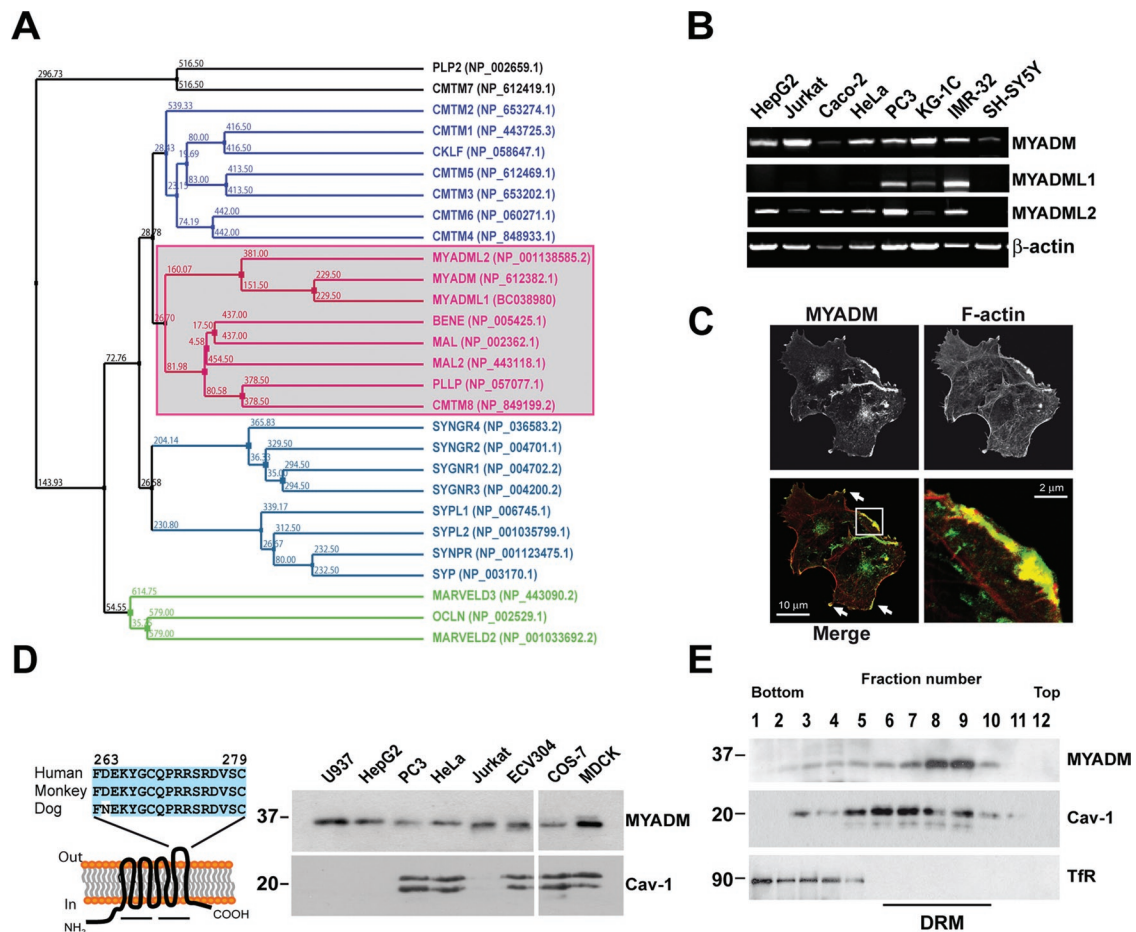
The tetra-spanning MARVEL (MAL and related proteins for vesicle trafficking and membrane link) membrane domain (Sanchez-Pulido *et al.*, 2002) is present in 28 human integral proteins grouped into different families, including the MAL family (Figure 1A). The best documented proteins of the MAL family contain four transmembrane segments expressed in a restricted range of tissues and are involved in specialized membrane-trafficking processes (Puertollano *et al.*, 1999; de Marco *et al.*, 2001, 2002; Bosse *et al.*, 2003). The other three members—MYADM, MYADM-like1 (MYADML1), and MYADM-like2 (MYADML2)—contain additional transmembrane segments and form an independent branch. To search for MAL-family proteins with ubiquitous expression plasma membrane localization and association with ordered membranes, we have analyzed the expression and distribution of the three MYADM proteins. An initial expression analysis of the *MYADM*, *MYADML1*, and *MYADML2* genes revealed that only *MYADM* expression was detected in all the human cell lines tested (Figure 1B). The widespread range of expression of *MYADM*, which is consistent with a previous analysis (Cui *et al.*, 2001), was confirmed by Northern blot analysis (Supplemental Figure S1A). Whereas the MYADML1 and MYADML2 proteins distributed intracellularly (Supplemental Figure S1B), as do other members of the MAL family (Puertollano *et al.*, 1999; de Marco *et al.*, 2001, 2002; Bosse *et al.*, 2003), MYADM localized to the plasma membrane (Figure 1C), where it overlapped extensively with F-actin in membrane ruffles. MYADM is the only

member of the MARVEL domain–containing superfamily that has two MARVEL domains (Figure 1D). The two MARVEL domains were necessary for targeting MYADM to the plasma membrane (Supplemental Figure S1C). Using a newly generated antibody (Supplemental Figure S1D), we confirmed at the protein level the widespread expression of MYADM (Figure 1D) and found that, similar to all the MAL family members analyzed to date, endogenous MYADM (Figure 1E) partitioned preferentially into detergent-resistant membranes (DRMs) enriched in compact membrane domains (Brown and Rose, 1992) as well as did exogenous MYADM-green fluorescent protein (GFP) (Supplemental Figure S1E). The domains organized by MYADM appear to be different from those organized by caveolin as a low level of colocalization was detected between both proteins (Supplemental Figure S1F). The widespread expression pattern of MYADM (Figure 1, B and D, and Supplemental Figure S1A), its presence at the plasma membrane (Figure 1C), and its partitioning into compact membranes (Figure 1E and Supplemental Figure S1E) are compatible with a general role of MYADM in raft-mediated events at the plasma membrane.

MYADM regulates cell spreading and migration

To gain insight into MYADM function, we adopted a loss-of-function strategy using specific shRNA or siRNA to generate transient knockdown (KD) of MYADM expression. First, cells were transfected with constructs expressing shRNA1 or shRNA2 that were targeted to the coding sequence or the 3′ untranslated region, respectively, of MYADM mRNA (Figure 2A). Cells expressing shRNA1 or shRNA2 were shown to maintain or severely reduce (~85–90%) MYADM levels, respectively, and were subsequently used as control or MYADM KD cells. We prepared stable transfectants expressing MYADM-GFP as a control of the specificity of shRNA2. MYADM-GFP transcript lacks the entire 3′ untranslated region of MYADM mRNA and thus is insensitive to shRNA2 (Figure 2A). Morphological analysis of MYADM KD cells revealed a reduction in the spreading area (Figure 2, B and C) and cell shape as measured by the elliptical factor (length/breadth) (Figure 2D) but not in the adhesion to the substratum (Figure 2E). Importantly, spreading and elongation defects were not observed in MYADM KD cells expressing exogenous MYADM-GFP (Figure 2, B–D). Further membrane dynamic analysis by time-lapse video microscopy revealed constant extension and retraction of the plasma membrane in subconfluent control cells undergoing random migration. In contrast, protrusive-retractile activity appeared remarkably lower at the edges of MYADM KD cells (Figure 2F). To test whether the defects in membrane dynamics affect the migratory capacity of the cells, we then compared control and MYADM KD cells in random migration assays (Figure 2G). The average velocity was significantly lower in MYADM KD cells than in control cells and in MYADM KD cells expressing MYADM-GFP (Figure 2H). In addition, the index of directionality (the net distance divided by the total distance traveled by the cell) measured on tracked cell trajectories diminished by ~50% in MYADM KD cells and was restored by expression of MYADM-GFP (Figure 2I).

To confirm the data obtained by shRNA expression in a second approach, HeLa cells were transiently transfected with specific siRNAs targeted to MYADM mRNA. siRNA1 did not significantly reduce MYADM expression and was chosen as a control siRNA whereas siRNA2 and siRNA3 knocked down MYADM levels by more than 90% and 80%, respectively, at 48 h posttransfection (Supplemental Figure S2A). The expression of siRNA2 recapitulated the effects on cell spreading and morphology and on velocity and directionality during random migration observed in shRNA2-transfected cells (Supplemental Figure S2, B–G). A milder effect on cell
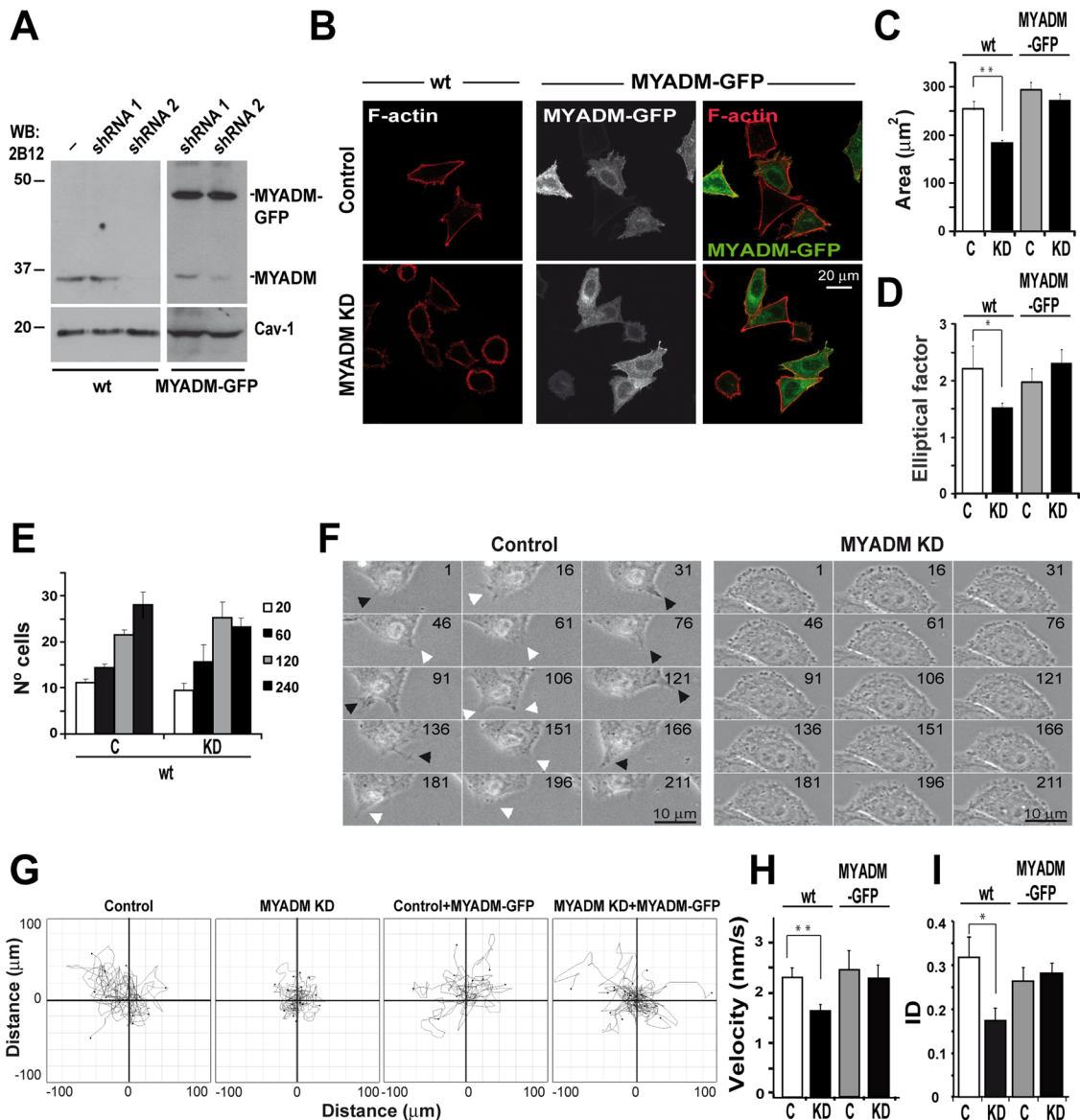
FIGURE 1: Characterization of the MYADM protein and analysis of its subcellular distribution. (A) Complete phylogenetic tree of human MARVEL domain-containing proteins. The sequences of the cytoplasmic amino- and carboxyl-terminal tails were not considered in the alignment used to generate the tree. The protein accession numbers of the corresponding sequences are indicated in brackets; the nucleotide accession number is indicated in the case of MYADML1. The MAL protein family is boxed. (B) RT-PCR analysis of the expression of the *MYADM, MYADML1,* and *MYADML2* genes in various human cell lines. (C) Cos-7 cells expressing human MYADM-GFP were stained for F-actin and analyzed by confocal microscopy. The enlargement shows the colocalization of MYADM and F-actin in the lamellipodia indicated in the boxed area. (D) Left panel: schematic model of the predicted structure of MYADM indicating the human peptide used for the generation of mAb2B12. The two lines below the model indicate the two MARVEL domains present in the MYADM molecule. Right panel: total membrane fractions from the indicated cell lines were subjected to immunoblotting with anti-MYADM mAb 2B12 or anti-caveolin-1 (Cav-1) antibodies. (E) HeLa cells were extracted with 1% Triton X-100 at 4°C and centrifuged to equilibrium in sucrose-density gradients. Aliquots from each fraction were immunoblotted for MYADM with 2B12 mAb or for caveolin-1 (Cav-1) and TfR used as markers of the DRM and soluble fractions, respectively.

morphology was observed in siRNA3-transfected cells (Supplemental Figure S2, C and D). Double staining of α-tubulin and F-actin revealed no major cytoskeletal alterations in siRNA2-transfected cells compared with control cells, although F-actin–enriched protrusions appeared to be reduced in extension and instead a thick F-actin belt decorated the cell periphery (Supplemental Figure S2B). Importantly, MYADM silencing in epithelial prostate PC3 cells reproduced the main findings obtained in HeLa cells (Supplemental Figure S2, H–K). In summary, the results in Figure 2 and Supplemental Figure S2 indicate that MYADM is necessary for normal cell spreading and migration.

MYADM regulates membrane condensation

To analyze the role of MYADM on membrane organization, we stained the cells with Laurdan. The Laurdan probe penetrates the cell membrane and aligns parallel to the phospholipids (Bagatolli
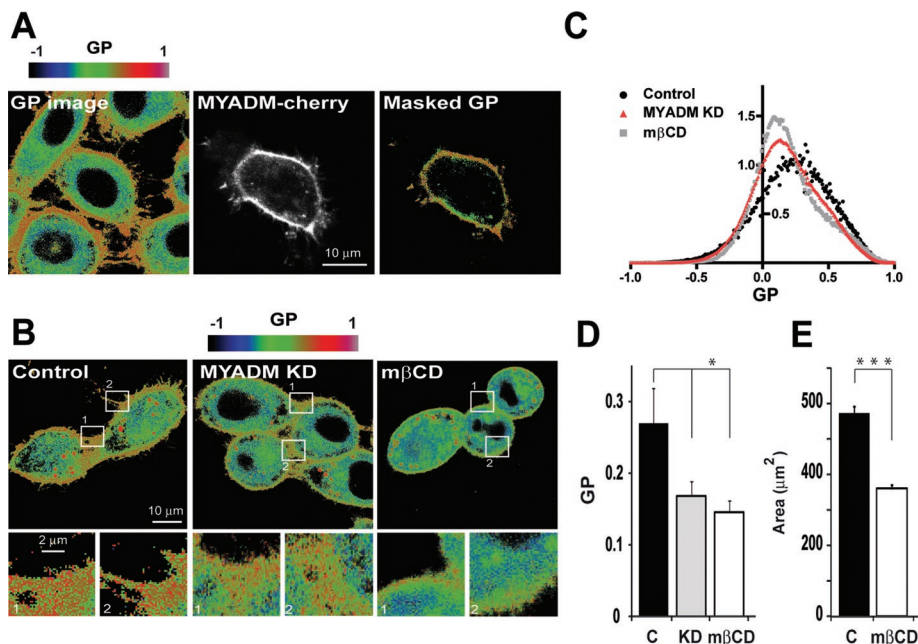
et al., 2003) undergoing a shift in its peak emission wavelength from ~500 nm in fluid membranes to ~440 nm in ordered membranes (Gaus et al., 2006). A normalized ratio of the two emission regions given by the general polarization (GP) index, which ranges between –1 and 1 provides a relative measure of membrane order. Analysis of Laurdan fluorescence under a two-photon confocal microscope has revealed that membranes at lamellipodial adhesions are highly ordered (Gaus et al., 2006a), consistent with previous findings showing the requirement of membrane rafts in these adhesive complexes for correct cell spreading (del Pozo et al., 2004). To analyze the order in MYADM-enriched membrane regions, we stained HeLa cells expressing MYADM-cherry with Laurdan and used the MYADM-cherry images to mask the GP images to visualize membrane order only at the regions containing MYADM. Using this procedure, we observed MYADM-enriched membrane protrusions to be highly ordered (Figure 3A). GP images were then used to compare membrane

FIGURE 2: MYADM regulates cell spreading and migration. (A) Normal HeLa cells (wt) or HeLa cells stably expressing MYADM-GFP were transfected or not with plasmids expressing shRNA1 or shRNA2 for 48 h. Cell extracts were then immunoblotted with anti-MYADM 2B12 mAb or anti-caveolin-1 (Cav-1) antibodies. (B–E) Control or MYADM KD cells expressing or not MYADM-GFP were plated onto glass coverslips. After 4 h, cells were stained for F-actin (B) and analyzed for their spreading area (C) and elliptical factor (D) or used immediately to determine adhesion kinetics by measuring the number of cells attached 20, 60, 120, or 240 min after plating (E). Twenty fields for each condition were analyzed in (E). (F) Control or MYADM KD cells were subjected to time-lapse videomicroscopy. Filled and unfilled arrowheads indicate extension and retraction of cell protrusions, respectively, at the plasma membrane. Numbers indicate time in minutes. (G–I) The movement of control or MYADM KD cells stably expressing or not MYADM-GFP was recorded by time-lapse videomicroscopy at 15-min intervals in random migration assays. The migration tracks of 12–16 cells from a representative experiment (G), the migration velocity of cells (H), and the index of directionality (ID) (I) are shown. The mean ± SEM from three independent experiments is shown in (C–E, H, and I). 120–150 cells per condition were analyzed in each experiment; *p < 0.05; **p < 0.01.

order in control MYADM KD cells and cells treated with the cholesterol-sequestering agent methyl-β-cyclodextrin by quantifying their respective GP value. Remarkably, MYADM KD significantly reduced the GP value concomitantly with cell rounding to a similar extent to the effect observed in cells treated with methyl-β-cyclodextrin (Figure 3, B–D). Thus our results indicate that MYADM regulates cell membrane condensation and that alteration of membrane condensation either by cholesterol depletion or MYADM silencing had a similar effect on cell spreading in HeLa cells (Figures 2C and 3E).

It is well documented that, in addition to GTP loading, correct targeting to the plasma membrane is required for efficient signaling of Rac1 (del Pozo et al., 2000). A close connection between Rac1 function and the presence of Rac1 in raft membranes has been established (del Pozo et al., 2004; Vilhardt and van Deurs, 2004). Laurdan staining confirmed that Rac1 preferentially localizes to ordered membranes with a high GP value (Figure 4A). Consistent with this observation, Rac1 was detected in MYADM-enriched DRMs isolated from HeLa cells, whereas RhoA or Cdc42 was excluded (Figure 4B).

FIGURE 3: MYADM KD reduces membrane condensation. (A) HeLa cells transiently expressing MYADM-cherry were stained with Laurdan for 30 min. Cells were then imaged for MYADM-cherry (middle panel) and for the Laurdan intensity in two channels (400–460 nm and 470–530 nm). Laurdan intensity images were converted to GP images and pseudocolored using the indicated scale (left panel) to represent low-to-high GP values (see scale). The masked GP image corresponding to the membrane regions labeled for MYADM-cherry was then obtained (right panel). (B–E) Control MYADM KD cells or normal cells the cholesterol content of which was reduced by treatment with 10 mM methyl-β-cyclodextrin (mβCD) for 15 min were stained with Laurdan. The GP distribution obtained in each case is represented as pseudocolored images (B, top panels) or normalized histograms (C). In (C), The x-axis represents GP values, and the y-axis shows the percentage of pixels found for each GP value. An enlargement of the boxed regions is also shown (B, bottom panels). The GP and spreading area are presented in (D) and (E), respectively. The mean ± SEM from three independent experiments is shown (D and E). 16–20 images for each condition (16–20 cells per image) were analyzed in three independent experiments; *p < 0.05; ***p < 0.001.

Remarkably, expression of constitutively active GFP-Rac1L61 increased lamellipodial extensions where MYADM and active Rac1 colocalized extensively (Figure 4C).

MYADM mediates Rac1 targeting to ordered membranes

To investigate the requirement for MYADM in targeting Rac1 to compact membranes, we compared the partitioning of Rac1 into DRMs of control and MYADM KD cells (Figure 5, A and B). The absence of MYADM expression clearly prevented Rac1 from segregating into DRMs compared with control cells. As a control for the specificity of the effect on Rac1, we observed that the partitioning of caveolin-1 and glycosylphosphatidylinositol-anchored protein CD59 was unaltered in MYADM KD cells. Importantly, the presence of Rac1 in DRMs was rescued by the expression of exogenous MYADM-GFP in MYADM KD cells (Figure 5, A and B). Paralleling the changes observed in the association of Rac1 with DRMs, the even distribution of Rac1 at the plasma membrane found in control cells changed to a more discrete pattern in MYADM KD cells (Figure 5C). Interestingly, the levels of neither active GTP-loaded Rac1 nor RhoA nor Cdc42 were significantly altered in MYADM KD cells (Figure 5D), indicating that MYADM regulates Rac1 by mediating its targeting to condensed membranes without affecting its state of GTP loading. These results evoked the effect previously observed for Rac1 activity in cells the membrane raft integrity of which was disrupted by cholesterol sequestration with methyl-β-cyclodextrin (del Pozo et al.,
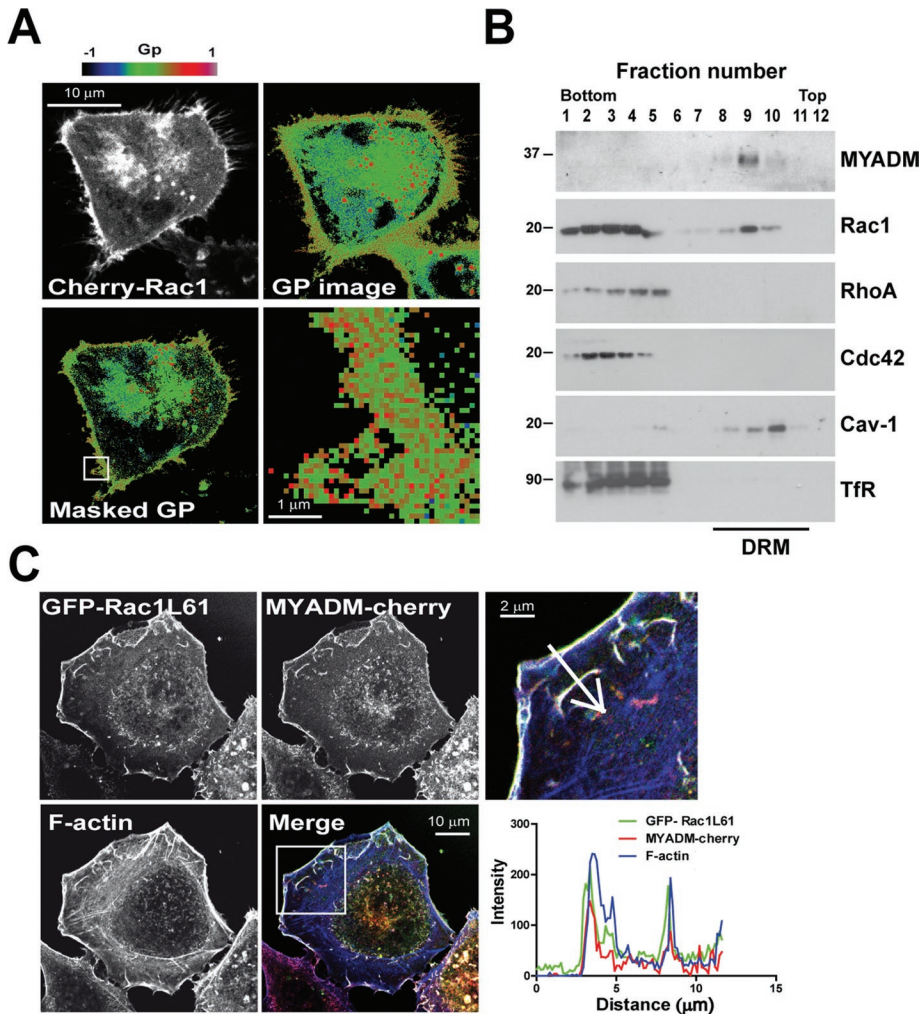
2004), and are consistent with previous findings showing not only that the state of GTP loading contributes to regulate the function of Rac1 but that its correct targeting to specialized raft membranes is also required (Michaely et al., 1999; Ghosh et al., 2002; del Pozo et al., 2004; Vilhardt and van Deurs, 2004; Golub and Pico, 2005).

To further investigate the role of MYADM in Rac1 function, we performed rescue-of-function experiments using MYADM KD or Rac1 KD cells expressing or not constitutively active Rac1L61 or MYADM-GFP, respectively (Figure 6A). Cell spreading, a hallmark of Rac1 function, was taken as the output (Figure 6B). As a control, we observed dominant-negative Rac1N17, which, similar to Rac1 KD, also reduced cell spreading and did not restore cell spreading in MYADM KD cells. Remarkably, active Rac1L61 increased cell spreading regardless of MYADM expression, whereas MYADM-GFP failed to restore the cell-spreading defect of the Rac1 KD cells. The effect of Rac1L61 expression in MYADM KD cells on cell spreading is consistent with previous observations indicating that constitutively active Rac1 can partially exert its functions without being properly targeted to the plasma membrane (del Pozo et al., 2000). In conclusion, the results in Figure 6 suggest that MYADM and Rac1 act on parallel pathways that lead to similar spreading outcomes.

DISCUSSION

The existence of cellular membrane heterogeneity has been widely reported by different experimental strategies that measure parameters as varied as stiffness (Wang et al., 2001; Roduit et al., 2008), microviscosity (Ghosh et al., 2002; Vasanji et al., 2004), or order (Gaus et al., 2006b; Jacobson et al., 2007). Mechanisms contributing to plasma membrane organization are however still poorly understood and somewhat controversial. The initial concept of preexisting auto-assembled lipid domains regulating membrane protein function has now evolved. Membrane rafts mediating localized signaling from different membrane regions are now envisaged as protein-based macromolecular assemblies that organize and are dependent on interactions with neighboring membrane lipids, such as cholesterol or phosphoinositides (Mayor et al., 2006).

All members of the MAL family characterized so far have a tissue-restricted pattern of expression and have been involved in raft-mediated specialized trafficking. The MAL protein founder of the family and its best characterized member appears to organize raft lipids as platforms for apical transport of influenza virus hemagglutinin (HA) in epithelial cells (Cheong et al., 1999; Puertollano et al., 1999; Magal et al., 2009) and Lck transport to the plasma membrane in T lymphocytes (Anton et al., 2008). In the absence of MAL expression, these cargoes are no longer able to partition into DRMs and travel to its destination, whereas exogenous expression of MAL restores both cargo trafficking and partitioning (Puertollano et al., 1999; Anton et al., 2008). Consistent with a role in the organization of raft lipids to generate condensed membranes (Puertollano et al., 1999;
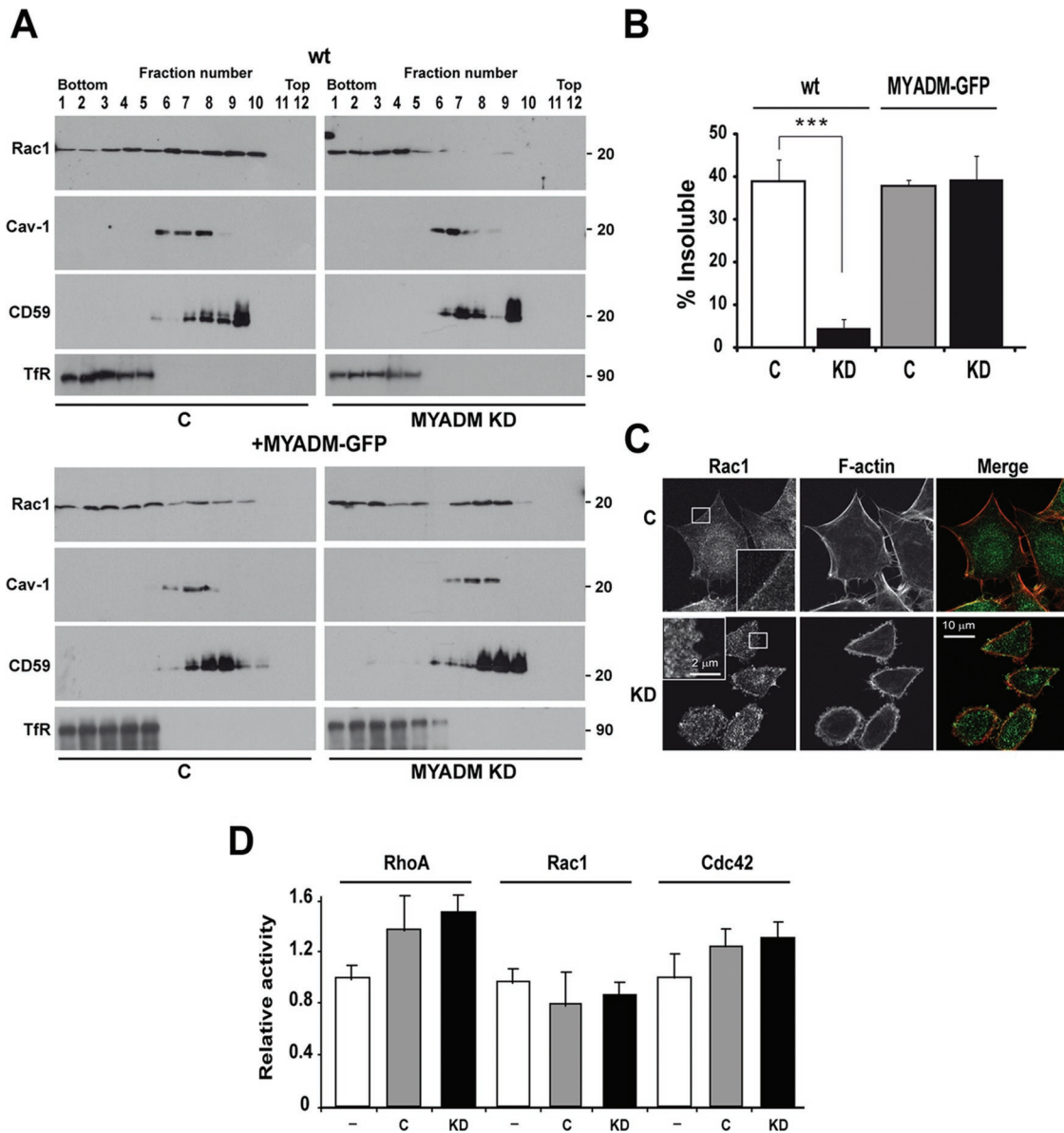
FIGURE 4: Rac1 colocalizes with MYADM at the plasma membrane and accumulates into compact membranes. (A) HeLa cells transiently expressing cherry-Rac1 were stained with Laurdan for 30 min. Cells were then imaged for cherry-Rac1 (top right panel) and for the Laurdan intensity in two channels (400–460 and 470–530 nm). Laurdan intensity images were converted to GP images and pseudocolored using the indicated scale (top left panel). The masked GP image corresponding to the membrane regions labeled for cherry-Rac1 was then obtained (bottom left panel). An enlargement of the boxed region is shown (bottom right panel). (B) HeLa cells were extracted with 0.2% Triton X-100 at 4°C, and the extracts were centrifuged to equilibrium in sucrose density gradients. The different fractions were analyzed for their content of the indicated proteins. The DRM fractions are indicated. (C) HeLa cells stably expressing MYADM-cherry were transfected with GFP-Rac1L61. After 24 h, cells were stained for F-actin and analyzed under a confocal microscope. An enlargement of the boxed region is shown. The plot shows the intensity of the staining of GFP-Rac1L61, MYADM-cherry, and F-actin along the line indicated by the arrow in the enlarged image.

expression of this MAL family member, which suggests a possible role of MYADM as an organizer of plasma membrane microdomains that play general or even housekeeping rather than specialized roles. In addition, MYADM has features such as displaying eight transmembrane segments organized as a tandem array of two MARVEL domains and being preferentially distributed at plasma membrane lamellipodia suggestive of a role organizing cell surface domains. Using different strategies to silence the MYADM gene in combination with the use of the membrane fluorescent Laurdan probe to measure membrane order, we have demonstrated here that MYADM regulates plasma membrane condensation. As a consequence, Rac1, which is loosely bound to ordered membranes in control cells, becomes excluded from those membranes in MYADM KD cells, whereas other more tightly attached proteins, such as caveolin-1 and CD59, are retained. Ectopic expression of MYADM in MYADM KD cells rescues Rac1 clustering into DRMs. Preventing Rac1 recruitment into DRMs has an effect on cell spreading and migration—a general cell function that is dependent on membrane condensation (Manes et al., 2003) or microviscosity (Ghosh et al., 2002; Vasanji et al., 2004). We cannot discount the possibility that the presence in rafts of proteins other than Rac1 might also be affected in MYADM KD cells. Nevertheless, based on the rescue experiments with constitutively active Rac1, we think that our hypothesis that the deficient targeting of Rac1 is a major cause of the defects of cell shape and motility observed in MYADM KD cells is a plausible one. Our results are consistent with previous reports showing that Rac1 is targeted to membrane-ordered domains upon adhesion and that integrity of cholesterol-enriched membranes is essential for Rac1 localization and cell migration (del Pozo et al., 2004; Palazzo et al., 2004). In our experimental model, pharmacological disruption of cholesterol membranes recapitulates the effect of MYADM knockdown.

Anton et al., 2008), Laurdan staining has shown that MAL clustering induces the formation of large domains with specific sorting properties (Magal et al., 2009). The four membrane-spanning segments of MAL constitute the MARVEL domain (Sanchez-Pulido et al., 2002), which is thought to play a role in membrane domain organization (Magal et al., 2009).

MYADM was identified as a gene the expression of which is upregulated during myeloid differentiation (Pettersson et al., 2000). Alteration of MYADM expression also has been found in human melanoma metastasis samples (de Wit et al., 2005) and during salt susceptibility–related hypertension (Yagil et al., 2005). Notwithstanding that MYADM levels may be modulated in different cell contexts, we and others have shown the widespread pattern of

On de-adhesion, Rac1 is translocated from surface cholesterol-enriched domains to an intracellular compartment. This trafficking is controlled by actin cholesterol and caveolin-1 (del Pozo et al., 2004, 2005). By following the glycolipid GM1 as a membrane raft marker, it also has been reported that subsequent cell adhesion regulates exocist- and Arf6-dependent traffic of membrane rafts from recycling endosomes to the cell surface. This process is in turn essential for proper integrin and growth factor signaling (Balasubramanian et al., 2007, 2010). In contrast, Rac1 activity also requires Arf6- and Rab5-dependent recycling from endosomes to plasma membrane necessary for cell migration (Radhakrishna et al., 1999; Zhang et al., 1999; del Pozo et al., 2004; Palamidessi et al., 2008). Given the parallels between membrane rafts and Rac1 dynamics upon adhesion, it can
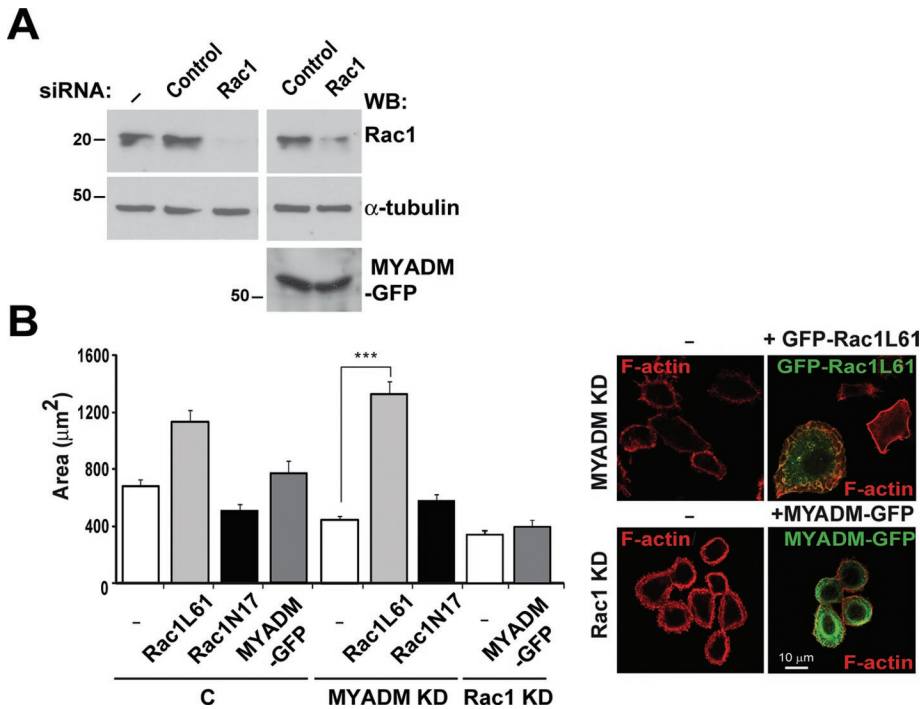
FIGURE 5: MYADM KD inhibits recruitment of Rac1 into compact membranes and alters the distribution of Rac1 at the plasma membrane. (A) Control or MYADM KD HeLa cells stably expressing or not MYADM-GFP were extracted with 0.2% Triton X-100 at 4°C, and the extracts were centrifuged to equilibrium in sucrose density gradients. The Rac1, caveolin-1, CD59, and TfR content of the different fractions was analyzed. (B) The histogram represents the percentage of insoluble Rac1 under the different conditions used in (A). (C) Control or MYADM KD cells were stained for endogenous Rac1 and F-actin. The insets show an enlargement of the boxed regions of the plasma membrane to illustrate the different pattern of distribution of Rac1 at the plasma membrane of control and MYADM KD cells. (D) The histograms show the levels of active Cdc42, Rac1, and RhoA in control and MYADM KD cells as determined in pull-down assays. The mean ± SEM from three independent experiments is shown in (B and D); ***$p < 0.001$.

be speculated that Rac1 trafficking from endosome compartments to cell surface during cell migration also occurs via ordered domains the presence of which in endosomes has been previously established (Puertollano et al., 2001; Masuyama et al., 2009; Nada et al., 2009). Formerly characterized members of the MAL family play central roles in specialized trafficking (Puertollano et al., 1999; de Marco et al., 2002; Anton et al., 2008) and have been found in this intracellular compartment (Puertollano et al., 2001). Thus it would be interesting to address in the future whether MYADM or other MAL family members could also participate in the endosome circuitry necessary for spatially restricted Rac1 function. It is of note that no physical link has been reported for these other proteins that determine Rac1 lo-

calization to membrane compartments such as Rab5 (Palamidessi et al., 2008) or caveolin-1 (del Pozo et al., 2005). Like that of MYADM, the role of these proteins is to regulate membrane compartments required for proper location and function of this GTPase.

MYADM expression is modulated in two processes highly related to cell migration, such as haematopoiesis and melanoma metastasis (Pettersson et al., 2000; de Wit et al., 2005). MYADM transcripts appear reduced in melanoma metastasis samples compared with benign nevocellular nevi (de Wit et al., 2005). This observation may apparently be inconsistent with a positive role proposed here of MYADM regulating Rac-dependent migration. Interestingly, melanoma cell lines have been studied as cell models that

FIGURE 6: Rescue-of-function experiments in MYADM KD or Rac1 KD cells. (A) Normal HeLa cells or HeLa cells stably expressing MYADM-GFP were transfected with control siRNA or siRNA targeted to Rac1 and processed for immunoblotting for Rac1, MYADM-GFP, and α-tubulin, which was used as a loading control. (B) Control MYADM KD or Rac1 KD cells were transfected with Rac1L61 or Rac1N17 or with MYADM-GFP, respectively, as indicated. Cells were then fixed, and their spreading area was determined 24 h later. The mean ± SEM is represented (left panel). Representative images of cells stained for F-actin of MYADM KD or Rac1 KD cells transfected or not with GFP-Rac1L61 or MYADM-GFP, respectively, are shown (right panel). At least three independent experiments were performed. 100–120 cells for each condition were analyzed; ***p < 0.001.

spontaneously adopt two distinct modes of movement during migration in three-dimensional extracellular matrices (Sanz-Moreno et al., 2008, 2010). The one called amoeboid or rounded movement is driven by high Rho activity and actomyosin contractility. This mode allows cells to squeeze forward through gaps present in the extracellular matrix in the absence of proteolytic activity. The alternative manner of tumor migration called mesenchymal or elongated is driven by extension of Rac-dependent lamellipodia and requires proteolytic processing of the extracellular matrix to allow cell movement across wider gaps. Both modes of three-dimensional migration are interconvertible; when Rac activity is kept low, cells switch to rounded migratory mode, which may confer additional plasticity to melanoma cells (Sanz-Moreno et al., 2010). In vivo comparative analysis of both modes of movement strongly suggests that amoeboid movement with low Rac activity favors invasion and metastasis of these cells (Sanz-Moreno et al., 2008). This observation is consistent with human melanoma metastasis samples containing cells with low levels of MYADM favoring invasive amoeboid movement and opens an attractive and unexplored possibility to MYADM playing a role in cell migration in a pathological context, such as cancer invasion.

In summary, unlike the previously characterized MAL members, MYADM is present at the plasma membrane and widely expressed, suggestive of a general raft-dependent role at the cell surface. Our results show that MYADM is necessary for correct membrane structure and appropriate targeting of Rac1 to specialized membrane rafts and subsequently for cell spreading and migration.

MATERIALS AND METHODS
Reagents
The rabbit polyclonal antibodies to caveolin-1 and the monoclonal antibody (mAb)s to RhoA, Rac1, and Cdc42 were obtained from BD Biosciences (San Jose, CA). Methyl-β-cyclodextrin and the mAb to α-tubulin or transferrin receptor (TfR) were purchased from Sigma-Aldrich (St. Louis, MO) and Zymed Laboratories (South San Francisco, CA), respectively. The anti-HA antibody 12CA5 and the anti-CD59 antibody MEM-43/5 were obtained from Roche (Indianapolis, IN) and Abcam (Cambridge, MA), respectively. Secondary goat antibodies coupled to Alexa 488 tetramethylrhodamine isothiocyanate–labeled phalloidin and the fluorescent probe Laurdan (6-acyl-2-dimethylaminon-apthalene) were purchased from Molecular Probes (Eugene, OR). Secondary antibodies coupled to horseradish peroxidase were obtained from Jackson ImmunoResearch (West Grove, PA).

Cell culture conditions
Human epithelial HeLa and PC3 cells were obtained from the American Type Culture Collection and maintained in Petri dishes in DMEM supplemented with 5% fetal bovine serum (Sigma-Aldrich), penicillin (50 U/ml), and streptomycin (50 μg/ml) at 37°C in an atmosphere of 5% CO_2/95% air.

DNA constructs, siRNA, and transfection conditions
The DNA constructs expressing MYADM tagged with HA, GFP, or cherry were generated by PCR using 5′ and 3′ oligonucleotide primers with the appropriate modifications and MYADM cDNA (IMAGE clone 3627858) as the template. The amplified MYADM coding sequence was cloned in-frame for the GFP or cherry open reading frame using the pEGFP-N1 or pmCherry-N1 plasmids (Clontech, Mountain View, CA) in the case of the fluorescent chimeras or in the PCR3.1 plasmid (Invitrogen, Carlsbad, CA) in the case of HA-tagged MYADM. The DNA constructs expressing GFP-tagged MYADML1 and MYADML2 were generated by cloning in pEGFP-N1 the DNA fragments obtained by PCR using 5′ and 3′ oligonucleotide-specific primers with the appropriate modifications and MYADML1 cDNA (IMAGE clone 5297847) or MYADML2 cDNA (IMAGE clone 5172276) as template, respectively. The DNA constructs in pEGFP-C1 or pm-Cherry-C1 for expression of GFP fused to the amino terminus of Rac1 Rac1L61 or Rac1N17 and the DNA constructs for expression of the Rho GTPase-binding domain of PAK1 (GST-PBD) or Rhotekin (GST-RBD) fused to GST were generous gifts from A. Ridley (King's College, London, UK). The 5′-ATGCCAGTGACGGTAACCCGC-3′ and 5′-GGTGCTGAGCTCACATCCA-3′ sequences, which target the AUG translation initiation site and immediately downstream sequences and the 3′ untranslated region of MYADM mRNA, respectively, separated by a short spacer (5′-TTCAAGAGA-3′) from their reverse complement were cloned under the control of the H1-RNA promoter in the pSuper DNA vector (Brummelkamp et al., 2002), thereby generating the shRNA1 and shRNA2 expression constructs.

Transfection of HeLa cells with plasmid DNA was performed by electroporation using an Electro Cell Manipulator 600 electroporation instrument (BTX, San Diego, CA). More than 90% of HeLa cells were transfected. To select stable transfectants, cells were treated with 0.5 mg/ml G-418 sulfate (Roche) for at least 4 wk after transfection. Cell clones were screened by immunoblot analysis. The clones that proved to be positive were maintained in drug-free medium. The siRNA duplexes 5′-ATCACTGGCTATATGGCC-3′ (siRNA1), 5′-GGT-GCTGAGCTCACATCCA-3′ (siRNA2), and 5′-GGTCTAAGACTCTC-CCAAG-3′ (siRNA3) targeted to MYADM mRNA and 5′-AGACG-GAGCUGUAGGUAAAUU-3′ targeted to Rac1 mRNA were purchased from Dharmacon (Chicago, IL). The sequences of all the siRNAs used were subjected to a Basic Local Alignment *Search* Tool (BLAST) search to ensure targeting specificity. siRNA was introduced into HeLa or PC3 cells using oligofectamine 2000 (Invitrogen).

Generation of mAbs to the MYADM protein
The peptide FDEKYGCQPRRSRDVSC corresponding to amino acids 263–279 of human MYADM was coupled to keyhole limpet hemocyanin (Thermo Fisher Scientific, Rockford, IL). Spleen cells from mice immunized with the peptide were fused to myeloma cells and plated onto microtiter plates. The hybridoma clone 2B12, which produces antibodies that recognize MYADM in membrane extracts from Cos-7 cells transiently expressing HA-tagged MYADM, was selected.

Laurdan staining
Labeling of live cells with the fluorescent probe Laurdan (5 μM) microscope calibration and two-photon microscopy were performed as described (Gaus *et al.*, 2003) using an LSM 710 NLO Multiphoton coupled to an AxioObserver inverted microscope (Carl Zeiss, Jena, Germany) with a 63× water objective NA 1.3. In brief, Laurdan was excited at 800 nm, and emission intensities were recorded simultaneously in the 400–460 nm and 470–530 nm ranges. Intensity images were converted into a GP index defined as I(400–460) – I(470–530) / I(400–460) + I(I(470–530), where I is the emission intensity as previously described (Gaus *et al.*, 2003). Images of a standard solution of 5 μM Laurdan in dimethyl sulfoxide at room temperature (22°C) were acquired to obtain the G factor as described (Gaus *et al.*, 2006b). The G factor was then used to correct the experimental GP values. GP values range from –1 (fluid domains) to +1 (highly ordered domains); membranes with GP values >0.3 are considered to be ordered membrane domains. The GP distributions and mean GP values were obtained from GP images normalized and represented using GraphPad Prism Software (San Diego, CA).

Confocal microscopy
Cells were fixed in 4% paraformaldehyde for 15 min, rinsed, and treated with 10 mM glycine for 5 min. The cells were then permeabilized with 0.2% Triton X-100, rinsed, and incubated with 3% bovine serum albumin in phosphate-buffered saline (PBS) for 15 min. Cells were incubated for 1 h with the indicated primary antibodies, rinsed several times, and incubated for 1 h with the appropriate Alexa 488–labeled secondary antibodies or with fluorescent phalloidin. Controls to assess labeling specificity included incubations with control primary antibodies or omission of the primary antibodies. Confocal fluorescence micrographs were taken using a Carl Zeiss LSM 510 microscope equipped with a 63× oil objective NA 1.3. Images were exported in TIFF format, and their brightness and contrast were optimized with Adobe Photoshop.

Random migration assays
Cells were plated onto fibronectin-coated coverslips and then immediately placed on the stage of a Carl Zeiss Axiovert 200 microscope equipped with a heated stage and CO_2 circulator to maintain cells at 37°C and 5% CO_2. Time-lapse analysis was performed at 15-min intervals for 17.5 h. Cell trajectories were manually tracked and analyzed from recorded images using MetaMorph 6.2r6 (Molecular Devices, Downingtown, PA) and ImageJ 1.43m software (http://rsb.info.nih.gov/ij). Briefly, the centroid of each cell was followed to calculate the index of directionality and velocity of individual cells correcting trajectories of overlapping cells during their movement and ruling out dividing cells from the analysis. We obtained similar results with both programs. Plots of directionality and the quantitative analysis of the elliptical factor and the area of the cells were obtained using in-house plug-ins for the ImageJ program.

RT-PCR and Northern blot analyses
The expression of MYADM, MYADML1, and MYADML2 in different cell lines was analyzed by RT-PCR using the Titan One-Tube kit (Roche) and 5′ and 3′ oligonucleotide primer pairs specific to each mRNA species. For Northern blot analysis, 20 μg of total RNA was hybridized under standard conditions to ^{32}P-labeled MYADM and β-actin cDNA probes.

DRM isolation
HeLa cells grown to confluence in 100-mm dishes were rinsed with PBS and lysed for 20 min in 1 ml of 25 mM Tris-HCl, pH 7.5; 150 mM NaCl, 5 mM EDTA, and 0.2% or 1% Triton X-100 as indicated at 4°C. The insoluble membrane fraction was isolated by centrifugation to equilibrium in a sucrose density gradient in a swinging bucket SW40 rotor (Beckman Coulter, Brea, CA) at 39,000 rpm (188,000 × *g*) for 20 h (Brown and Rose, 1992). Twelve 1-ml fractions were harvested from the bottom to the top of the centrifuge tube, and equivalent aliquots were subjected to immunoblot analysis with the appropriate antibodies.

Pull-down assays
HeLa cells were lysed in 50 mM Tris-HCl, pH 7.4; 1 mM $MgCl_2$; 2 mM EDTA; 300 mM NaCl; 0.5% Nonidet P-40; and 10% glycerol containing a cocktail of protease inhibitors. Recombinant GST, GST-PBD, or GST-RBD proteins (10 μg) immobilized on GSH-Sepharose beads (GE Life Sciences, Piscataway, NJ) were incubated with the lysates for 1 h at 4°C in lysis buffer containing 10 mM $MgCl_2$. The beads were washed three times in interaction buffer, and bound proteins were analyzed by immunoblotting with anti-RhoA-Rac1 or -Cdc42 mAbs.

Bioinformatics analysis
Protein information was retrieved from Universal Protein Resource (UniProt; http://www.expasy.uniprot.org) using the Batch Retrieval function available at the Protein Information Resource Web site (http://pir.georgetown.edu). Protein sequences were aligned, and the resulting phylogenetic tree of MARVEL domain-containing proteins was derived using JALVIEW (University of Dundee, UK).

Statistical analysis
Quantitative data are expressed as the mean ± SEM. A paired Student's *t* test was used to establish the statistical significance of differences between the means.

REFERENCES

Anton O, Batista A, Millan J, Andres-Delgado L, Puertollano R, Correas I, Alonso MA (2008). An essential role for the MAL protein in targeting Lck to the plasma membrane of human T lymphocytes. J Exp Med 205, 3201–3213.

Bagatolli LA, Sanchez SA, Hazlett T, Gratton E (2003). Giant vesicles Laurdan and two-photon fluorescence microscopy: evidence of lipid lateral separation in bilayers. Meth Enzymol 360, 481–500.

Balasubramanian N, Meier JA, Scott DW, Norambuena A, White MA, Schwartz MA (2010). RalA-exocyst complex regulates integrin-dependent membrane raft exocytosis and growth signaling. Curr Biol 20, 75–79.

Balasubramanian N, Scott DW, Castle JD, Casanova JE, Schwartz MA (2007). Arf6 and microtubules in adhesion-dependent trafficking of lipid rafts. Nat Cell Biol 9, 1381–1391.

Bosse F, Hasse B, Pippirs U, Greiner-Petter R, Muller HW (2003). Proteolipid plasmolipin: localization in polarized cells regulated expression and lipid raft association in CNS and PNS myelin. J Neurochem 86, 508–518.

Brown DA, Rose JK (1992). Sorting of GPI-anchored proteins to glycolipid-enriched membrane subdomains during transport to the apical cell surface. Cell 68, 533–544.

Brummelkamp TR, Bernards R, Agami R (2002). A system for stable expression of short interfering RNAs in mammalian cells. Science 296, 550–553.

Cheong KH, Zacchetti D, Schneeberger EE, Simons K (1999). VIP17/MAL, a lipid raft-associated protein, is involved in apical transport in MDCK cells. Proc Natl Acad Sci USA 96, 6241–6248.

Cui W, Yu L, He H, Chu Y, Gao J, Wan B, Tang L, Zhao S (2001). Cloning of human myeloid-associated differentiation marker (MYADM) gene whose expression was up-regulated in NB4 cells induced by all-trans retinoic acid. Mol Biol Rep 28, 123–138.

de Marco MC, Kremer L, Albar JP, Martinez-Menarguez JA, Ballesta J, Garcia-Lopez MA, Marazuela M, Puertollano R, Alonso MA (2001). BENE a novel raft-associated protein of the MAL proteolipid family interacts with caveolin-1 in human endothelial-like ECV304 cells. J Biol Chem 276, 23009–23017.

de Marco MC, Martin-Belmonte F, Kremer L, Albar JP, Correas I, Vaerman JP, Marazuela M, Byrne JA, Alonso MA (2002). MAL2 a novel raft protein of the MAL family is an essential component of the machinery for transcytosis in hepatoma HepG2 cells. J Cell Biol 159, 37–44.

de Wit NJ, Rijntjes J, Diepstra JH, van Kuppevelt TH, Weidle UH, Ruiter DJ, van Muijen GN (2005). Analysis of differential gene expression in human melanocytic tumour lesions by custom made oligonucleotide arrays. Br J Cancer 92, 2249–2261.

del Pozo MA, Alderson NB, Kiosses WB, Chiang HH, Anderson RG, Schwartz MA (2004). Integrins regulate Rac targeting by internalization of membrane domains. Science 303, 839–842.

del Pozo MA, Balasubramanian N, Alderson NB, Kiosses WB, Grande-Garcia A, Anderson RG, Schwartz MA (2005). Phospho-caveolin-1 mediates integrin-regulated membrane domain internalization. Nat Cell Biol 7, 901–908.

del Pozo MA, Price LS, Alderson NB, Ren XD, Schwartz MA (2000). Adhesion to the extracellular matrix regulates the coupling of the small GTPase Rac to its effector PAK. EMBO J 19, 2008–2014.

Gaus K, Gratton E, Kable EP, Jones AS, Gelissen I, Kritharides L, Jessup W (2003). Visualizing lipid structure and raft domains in living cells with two-photon microscopy. Proc Natl Acad Sci USA 100, 15554–15559.

Gaus K, Le Lay S, Balasubramanian N, Schwartz MA (2006a). Integrin-mediated adhesion regulates membrane order. J Cell Biol 174, 725–734.

Gaus K, Zech T, Harder T (2006b). Visualizing membrane microdomains by Laurdan 2-photon microscopy. Mol Membr Biol 23, 41–48.

Ghosh PK, Vasanji A, Murugesan G, Eppell SJ, Graham LM, Fox PL (2002). Membrane microviscosity regulates endothelial cell motility. Nat Cell Biol 4, 894–900.

Golub T, Pico C (2005). Spatial control of actin-based motility through plasmalemmal PtdIns(4,5)P2-rich raft assemblies. Biochem Soc Symp 72, 119–127.

Heasman SJ, Ridley AJ (2008). Mammalian Rho GTPases: new insights into their functions from in vivo studies. Nat Rev Mol Cell Biol 9, 690–701.

Jacobson K, Mouritsen OG, Anderson RG (2007). Lipid rafts: at a crossroad between cell biology and physics. Nat Cell Biol 9, 7–14.

Lingwood D, Simons K (2010). Lipid rafts as a membrane-organizing principle. Science 327, 46–50.

Magal LG, Yaffe Y, Shepshelovich J, Aranda JF, de Marco MdC, Gaus K, Alonso MA, Hirschberg K (2009). Clustering and lateral concentration of raft lipids by the MAL protein. Mol Biol Cell 20, 3751–3762.

Manes S, Ana Lacalle R, Gomez-Mouton C, Martinez AC (2003). From rafts to crafts: membrane asymmetry in moving cells. Trends Immunol 24, 320–326.

Masuyama N, Kuronita T, Tanaka R, Muto T, Hirota Y, Takigawa A, Fujita H, Aso Y, Amano J, Tanaka Y (2009). HM1.24 is internalized from lipid rafts by clathrin-mediated endocytosis through interaction with alpha-adaptin. J Biol Chem 284, 15927–15941.

Mayor S, Viola A, Stan RV, del Pozo MA (2006). Flying kites on slippery slopes at Keystone. Symposium on Lipid Rafts and Cell Function. EMBO Rep 7, 1089–1093.

Michaely PA, Mineo C, Ying YS, Anderson RG (1999). Polarized distribution of endogenous Rac1 and RhoA at the cell surface. J Biol Chem 274, 21430–21436.

Nada S, Hondo A, Kasai A, Koike M, Saito K, Uchiyama Y, Okada M (2009). The novel lipid raft adaptor p18 controls endosome dynamics by anchoring the MEK-ERK pathway to late endosomes. EMBO J 28, 477–489.

Palamidessi A, Frittoli E, Garre M, Faretta M, Mione M, Testa I, Diaspro A, Lanzetti L, Scita G, Di Fiore PP (2008). Endocytic trafficking of Rac is required for the spatial restriction of signaling in cell migration. Cell 134, 135–147.

Palazzo AF, Eng CH, Schlaepfer DD, Marcantonio EE, Gundersen GG (2004). Localized stabilization of microtubules by integrin- and FAK-facilitated Rho signaling. Science 303, 836–839.

Pettersson M, Dannaeus K, Nilsson K, Jonsson JI (2000). Isolation of MYADM a novel hematopoietic-associated marker gene expressed in multipotent progenitor cells and up-regulated during myeloid differentiation. J Leukoc Biol 67, 423–431.

Puertollano R, Martin-Belmonte F, Millan J, de Marco MC, Albar JP, Kremer L, Alonso MA (1999). The MAL proteolipid is necessary for normal apical transport and accurate sorting of the influenza virus hemagglutinin in Madin-Darby canine kidney cells. J Cell Biol 145, 141–151.

Puertollano R, Martinez-Menarguez JA, Batista A, Ballesta J, Alonso MA (2001). An intact dilysine-like motif in the carboxyl terminus of MAL is required for normal apical transport of the influenza virus hemagglutinin cargo protein in epithelial Madin-Darby canine kidney cells. Mol Biol Cell 12, 1869–1883.

Radhakrishna H, Al-Awar O, Khachikian Z, Donaldson JG (1999). ARF6 requirement for Rac ruffling suggests a role for membrane trafficking in cortical actin rearrangements. J Cell Sci 112, 855–866.

Ridley AJ, Schwartz MA, Burridge K, Firtel RA, Ginsberg MH, Borisy G, Parsons JT, Horwitz AR (2003). Cell migration: integrating signals from front to back. Science 302, 1704–1709.

Roduit C, Van Der Goot FG, De Los Rios P, Yersin A, Steiner P, Dietler G, Catsicas S, Lafont F, Kasas S (2008). Elastic membrane heterogeneity of living cells revealed by stiff nanoscale membrane domains. Biophys J 94, 1521–1532.

Rolfe BE, Worth NF, World CJ, Campbell JH, Campbell GR (2005). Rho and vascular disease. Atherosclerosis 183, 1–16.

Sanchez-Pulido L, Martin-Belmonte F, Valencia A, Alonso MA (2002). MARVEL: a conserved domain involved in membrane apposition events. Trends Biochem Sci 27, 599–601.

Sanz-Moreno V, Gadea G, Ahn J, Paterson H, Marra P, Pinner S, Sahai E, Marshall CJ (2008). Rac activation and inactivation control plasticity of tumor cell movement. Cell 135, 510–523.

Sanz-Moreno V, Marshall CJ (2010). The plasticity of cytoskeletal dynamics underlying neoplastic cell migration. Curr Opin Cell Biol 22, 690–696.

Simons K, Ikonen E (1997). Functional rafts in cell membranes. Nature 387, 569–572.

Vasanji A, Ghosh PK, Graham LM, Eppell SJ, Fox PL (2004). Polarization of plasma membrane microviscosity during endothelial cell migration. Dev Cell 6, 29–41.

Vilhardt F, van Deurs B (2004). The phagocyte NADPH oxidase depends on cholesterol-enriched membrane microdomains for assembly. EMBO J 23, 739–748.

Wang Q, Chiang ET, Lim M, Lai J, Rogers R, Janmey PA, Shepro D, Doerschuk CM (2001). Changes in the biomechanical properties of neutrophils and endothelial cells during adhesion. Blood 97, 660–668.

Yagil C, Hubner N, Monti J, Schulz H, Sapojnikov M, Luft FC, Ganten D, Yagil Y (2005). Identification of hypertension-related genes through an integrated genomic-transcriptomic approach. Circ Res 96, 617–625.

Yamazaki D, Kurisu S, Takenawa T (2005). Regulation of cancer cell motility through actin reorganization. Cancer Sci 96, 379–386.

Zhang Q, Calafat J, Janssen H, Greenberg S (1999). ARF6 is required for growth factor- and rac-mediated membrane ruffling in macrophages at a stage distal to rac membrane targeting. Mol Cell Biol 19, 8158–8168.